Resource Management and Cell Planning in Millimeter-Wave Overlaid Ultra-Dense Cellular Networks

Jihong Park, Seong-Lyun Kim, and Jens Zander

Abstract—**This paper proposes a cellular network exploiting millimeter-wave (mmWave) and ultra-densified base stations (BSs) to achieve the far-reaching 5G aim in downlink average rate. The mmWave overlaid network however incurs a pitfall that its ample data rate is only applicable for downlink transmissions due to the implementation difficulty at mobile users, leading to an immense difference between uplink and downlink rates. We therefore turn our attention not only to maximize downlink rate but also to ensure the minimum uplink rate. With this end, we firstly derive the mmWave overlaid ultra-dense cellular network spectral efficiencies for both uplink and downlink cases in closed forms by using stochastic geometry via a lower bound approximation. In a practical scenario, such tractable results of the proposed network reveal that incumbent micro-wave (μWave) cellular resource should be mostly dedicated to uplink transmissions in order to correspond with the mmWave downlink rate improvement. Furthermore, increasing uplink rate via μWave BS densification cannot solely cope with the mmWave downlink/uplink rate asymmetry, and thus requires additional μWave spectrum in 5G cellular networks.**

Index Terms—**Ultra-dense cellular networks, millimeter-wave, heterogeneous cellular networks, radio resource management, cell planning, stochastic geometry, coverage process, Boolean model.**

I. Introduction

The scarcity of cellular frequency for achieving the 1,000x higher data rate in 5G brings about exploiting the millimeter-wave (mmWave) frequency band having hundreds times more spectrum amount [1]. This approach however has two major drawbacks. Firstly, mmWave signals are vulnerable to physical blockages, yielding severe distance attenuation. Secondly, the use of extremely wide mmWave bandwidth makes uplink mmWave transmissions at mobiles demanding due to high peak-to-average-ratio (PAPR) [2], leading to significant rate difference between uplink and downlink.

To compensate both drawbacks, we consider base station (BS) ultra-densification. It is another promising way to enhance the data rate by increasing per-user available resource amount [3] and even by improving per-user average spectral efficiency [4], [5]. This study combines such complementary two methods, and thereby proposes a mmWave overlaid ultra-dense cellular network.

The proposed network in distinction from other existing heterogeneous networks is the asymmetric uplink and downlink structure where mmWave band only operates for downlink transmissions (see Fig. 1). The reason is even the state-of-the-art mmWave supporting power amplifiers are low energy efficient, so uplink mmWave transmissions are demanding of mobile users [2]. Uplink communication therefore solely resorts to the current micro-wave (μWave) cellular frequency

band. Due to the scarcity of the μWave spectrum, the uplink data rate cannot keep up with the rising ample downlink data rate as mmWave resource and BS densification grow, which may hinder consistent user experiences. This uplink/downlink asymmetry motivates to turn our attention toward assuring the minimum uplink average rate, and engenders the mmWave overlaid cellular network design problem: *how to maximize the downlink average rate while guaranteeing a target uplink average rate*.

We answer this question from the radio resource management and cell planning perspectives. Exploiting stochastic geometry and the technique proposed in our preliminary work [5], we derive downlink mmWave and uplink/downlink μWave spectral efficiencies in closed forms. Utilizing these tractable results, we analyze the impacts of resource management and cell planning on downlink and uplink average rates. Such results provide the design guidelines of the mmWave overlaid ultra-dense cellular networks.

The main contributions of this paper are listed as follows.

1. *Most of the μWave resource should be dedicated to uplink transmissions* in order to guarantee the uplink average rate by at least 3% of the downlink rate in a practical scenario where μWave and mmWave resource amounts respectively are 20 MHz and 500 MHz [6] (see Proposition 3 and Fig. 6). This runs counter to the current resource allocation trend that is likely to allocate more resource to downlink transmissions [7].

2. To achieve the ever-growing downlink average rate while guaranteeing uplink average rate, *densifying μWave BS cannot be a sole remedy in practice* (see Proposition 4), *but should be in conjunction with procuring more μWave spectrums* (see Corollary 2). The reason behind is more spectrum amount linearly increases the uplink average rate while BS densification logarithmically increases the rate (see Proposition 1).

3. The spectral efficiencies in uplink/downlink μWave (see Proposition 1) and downlink mmWave bands (see Proposition 2) under an ultra-dense environment are derived in closed forms via a lower bound approximation, which reveals *BS densification logarithmically increases the spectral efficiency*.

Due to the lack of the space, the omitted proofs of propositions and lemmas are deferred to: *http://tiny.cc/jhparkgc15pf*.

II. System Model

A. Milimeter-Wave Overlaid Cellular Network

The proposed network comprises: (i) mmWave BSs whose locations follow a two-dimensional homogeneous Poisson point process (PPP) Φ_m with density λ_m; and (ii) μWave BSs whose coordinates follow a homogeneous PPP Φ_μ with density λ_μ, independent of Φ_m. Due to the implementational difficulty of mmWave transmissions at mobile users, mmWave

J. Park and S.-L. Kim are with Dept. of Electrical & Electronic Engineering, Yonsei University, Seoul, Korea (email: jhpark.james@yonsei.ac.kr, slkim@yonsei.ac.kr).

J. Zander is with Wireless@KTH, KTH – The Royal Institute of Technology, Stockholm, Sweden (email: jensz@kth.se).
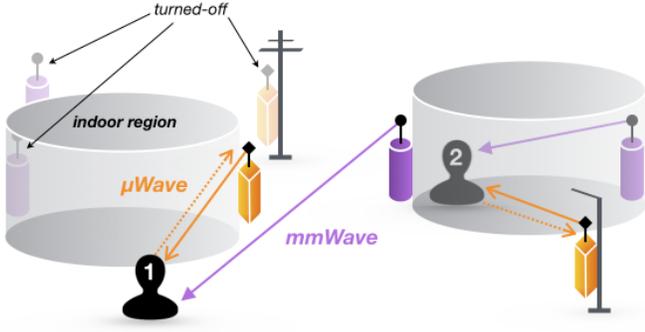
Fig. 1. Illustration of a mmWave overlaid cellular network where downlink signals are transmitted via both mmWave and μWave bands whereas the uplink only via μWave band. Indoor region is not penetrated by mmWave but μWave signals. Users associate with the nearest non-blocked mmWave BSs (outdoor user 1 associates with a farther mmWave BS than the nearest indoor BS) as well as with the nearest μWave BSs without any restriction (indoor user 2 associates with the outside nearest μWave BS). The BSs having no serving users are turned-off.

BS only supports downlink mode whereas μWave BS provides both downlink and uplink modes. Uplink transmissions are therefore resort to solely depend on μWave BSs. A BS having no serving user is turned off (see the transparent BSs in Fig. 1).

Mobile user coordinates independently follow a homogeneous PPP Φ_u with density λ_u. Without loss of generality, Φ_u represents both downlink and uplink users. Users receive downlink signals via both mmWave and μWave simultaneously [7] while transmitting uplink signals only via μWave. Specifically, downlink users associate with their nearest non-blocked mmWave BSs, and also independently with their nearest μWave BSs as in [7], [8]. Uplink users associate with the nearest μWave BSs that are identical with their μWave downlink associated BSs but the mmWave associated BSs. Such associations are visually shown by Fig. 1.

B. Indoor/Outdoor Model

Consider indoor regions whose boundaries are mmWave impenetrable walls. Followed by a Boolean model [9], the indoor regions are regarded as uniformly distributed circles having radius R with density λ_g. For simplicity without loss of generality, assume the indoor regions always guarantee line-of-sight (LOS) communications. Additionally, we neglect the overlapping indoor regions that can be compensated by a sufficiently large network. Note that μWave signals are not affected by the indoor walls thanks to their high diffraction and penetration characteristics. The indoor complementary regions are outdoor regions.

C. Channel Model

Our channel model is three-fold in order to capture the different propagation behaviors of outdoor/indoor mmWave and μWave signals.

1) Outdoor mmWave Channel: A mmWave antenna array directionally transmits a downlink signal with unity power to its associated user, and the signal experiences path loss attenuation with the exponent $\alpha_m > 2$ as well as Rayleigh fading with unity mean. The transmitted directional beam has

the main lobe angle θ (radian), and the received signal powers at the same distances within θ are assumed to be identical.

Users are able to receive mmWave signals only if there exist no indoor walls along the paths to their associated BSs. To specify this event, consider a typical user U_0 located at the origin and an arbitrary BS at X_i with distance r_i. Let $\mathbf{u_i}$ denote the opposite unit direction vector of the signal transmission direction from X_i, defined as $|X_i|/r_i$. Define $L(\mathbf{u_i})$ as the non-blockage distance indicating the line length from U_0 with the direction $\mathbf{u_i}$ to the point when the line firstly intersects an impenetrable indoor wall. A user then can receive a transmitted signal if the condition $L(\mathbf{u_i}) > r_i$ holds.

For interfering links, we consider the interferers as the undesired active BSs whose serving directions, the main lobe centers, pointing to U_0. It leads to Θ_i antenna gain, which is an increasing function of θ as well as the number of the BS's serving users. At U_0 when located outside the indoor regions, the corresponding mmWave signal-to-interference-plus-noise (SINR) is represented as:

$$\mathsf{SINR}_{m.out} := \begin{cases} \frac{\eta r^{-\alpha_m}}{\sum_{i \in \Phi_{m.out}} \Theta_i \eta_i r_i^{-\alpha_m} + \sigma^2} & \text{if } L(\mathbf{u}) > r \\ 0 & \text{otherwise} \end{cases} \quad (1)$$

where $\Phi_{m.out}$ indicates active non-blocked mmWave interfering outdoor BSs, η_i fading power, and σ^2 noise power.

2) Indoor mmWave Channel: Path loss exponent is set as 2 since there is no mmWave blockages within indoor regions as described in Section II-B. The rest of the settings are the same as in the case of the outdoor mmWave. At U_0 when located within indoor regions, the mmWave SINR is given as:

$$\mathsf{SINR}_{m.in} := \frac{\eta r^{-2}}{\sum_{i \in \Phi_{m.in}} \Theta_i \eta_i r_i^{-2} + \sigma^2} \quad (2)$$

where $\Phi_{m.in}$ denotes active mmWave interfering indoor BSs.

3) μWave Channel: A transmitted signal with unity power experiences path loss attenuation with the exponent $\alpha_\mu > 2$ as well as Rayleigh fading, resulting in the fading gain g that follows an exponential distribution with mean 1. At U_0, the μWave SINR is given as:

$$\mathsf{SINR}_\mu := \frac{g r^{-\alpha_\mu}}{\sum_{i \in \Phi_\mu} g_i r_i^{-\alpha_\mu} + \sigma^2} \quad (3)$$

where Φ_μ represents active μWave interfering BSs.

III. SPECTRAL EFFICIENCY IN ULTRA-DENSE CELLULAR NETWORKS

This section derives closed-form mmWave and μWave spectral efficiencies, defined as ergodic capacity $\mathsf{E} \log[1 + \mathsf{SINR}]$ in units of nats/sec/Hz (1bit $\approx$ 0.693 nats), to be utilized for resource allocation in Section IV. For brevity, we consider a downlink network in this section unless otherwise noted.

A. Ultra-Densification Effect

Throughout this study, an ultra-dense environment is of our interest. The ultra-densification implies BS density is much larger than user density such that the distance to an interfering BS at a typical receiver can be approximated by the distance to the interfering BS's nearest user.

To be more rigorous, define active probability p_a that an arbitrary μWave BS is turned-on, i.e. serving at least a single user within its coverage. According to Proposition 1 in [10],

$$p_a = \left\{ 1 - (1 + 3.5^{-1} \lambda_u / \lambda_\mu)^{-3.5} \right\} \overset{(a)}{\approx} \lambda_u / \lambda_\mu \quad (4)$$
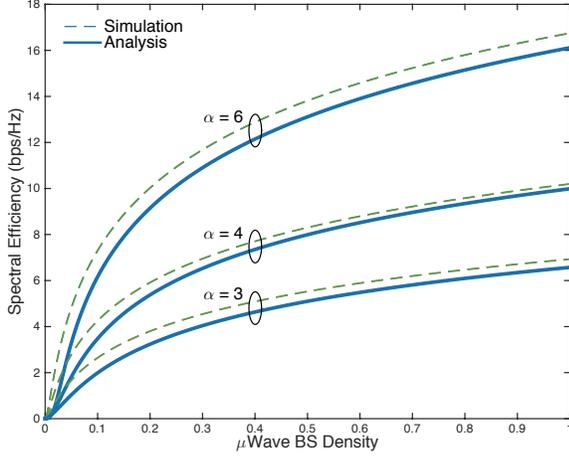
Fig. 2. Spectral efficiency of a typical downlink (or uplink) μWave user for path loss exponents $\alpha = 3$, 4, and 6 where user density λ_{u} is set as 0.02. Compared to the simulation curve when $\alpha = 4$, the analytic curve achieves: 81.75%, 90.9%, and 97.96% for $\lambda_\mu = 0.1$, 0.2, and 1 respectively.
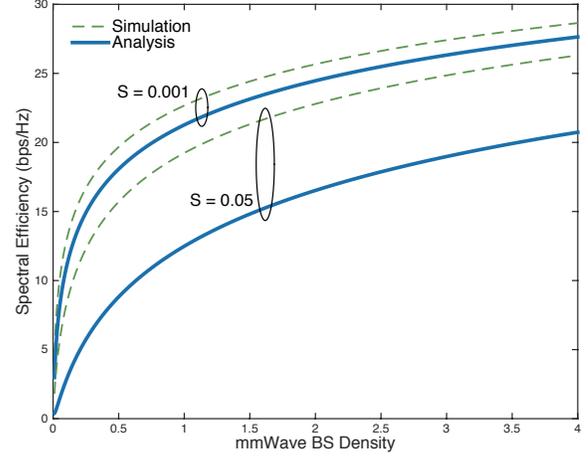

Fig. 3. Spectral efficiency of a typical *outdoor* downlink mmWave user for the outdoor path loss exponent $\alpha_{\mathrm{m}} = 5.76$ [1] where user density $\lambda_{\mathrm{u}} = 0.02$, indoor region density $\lambda_g = 0.1$, and main lobe beam width $10°$.

where (a) follows from Taylor expansion for $\lambda_\mu \gg \lambda_{\mathrm{u}}$.

This tendency in ultra-dense networks results in the active BS density $p_a\lambda_\mu$ converging to λ_{u}. The result implies ultra-densification enables to increase the received signal power without incurring any interference increment since interference is delimited by user density independent of the BS densification. The same tendency applies to the mmWave BS active probability, so p_a henceforth denotes both μWave and mmWave active probabilities.

B. μWave Spectral Efficiency

This section derives the tractable but accurate lower bounds of uplink and downlink μWave spectral efficiencies. Firstly, consider uplink spectral efficiency that is deemed difficult to be analyzed in a stochastic geometric point of view.

To specify the difficulty, we compare downlink and uplink scenarios. In a downlink case at U_0, all interfering BSs are farther than the associated BS. In an uplink case at a typical BS X_0, on the other hand, interfering users may be located closer than the associated user U_0 since the nearest association is not determined by X_0 but users. This distance disorder of uplink interferers and U_0 makes the uplink aggregate interference analysis complicated.

Ultra-dense environment however allows to detour the distance disorder problem by enabling an uplink-downlink reciprocity thanks to short user-to-active BS distances, which leads to the following Lemma.

Lemma 1. *(Uplink–Downlink Reciprocity)* For $\lambda_\mu \gg \lambda_{\mathrm{u}}$, uplink and downlink μWave spectral efficiencies are identical.

Secondly, consider downlink μWave spectral efficiency. Its closed-form result has been derived in our preliminary work [5], but is restated here for the integrity of this study in the following Proposition.

Proposition 1. *(Uplink/Downlink μWave)* At U_0 for $\lambda_\mu \gg \lambda_{\mathrm{u}}$, uplink (or downlink) μWave spectral efficiency γ_μ is lower bounded as follows.

$$\gamma_\mu > \log\left(1 + \left[\frac{\lambda_\mu}{\rho_\mu \lambda_{\mathrm{u}}}\right]^{\alpha_\mu/2}\right) \tag{5}$$

where $\rho_\mu := \int_0^\infty 1/(1 + u^{\alpha_\mu/2})du$

The result indicates that increasing BS density logarithmically improves the μWave spectral efficiency. The tightness of the proposed lower bound is numerically verified by Fig. 2. The figure also illustrates increasing path loss exponent enhances the spectral efficiency since its resultant interference reduction dominates the desired signal attenuation under an interference-limited regime as expected in [10].

C. mmWave Spectral Efficiency

This section derives the downlink mmWave spectral efficiencies under outdoor and indoor environments. A notable mmWave characteristic in distinction from the preceding μWave analysis is indoor wall impenetrability. Its impact on the mmWave spectral efficiency is captured by a single indoor region area S defined as πR^2. We confine to considering a large outdoor region compared to indoor region, i.e. small S. Specifically, S is sufficiently small in such a way that each indoor region contains at most a single user, leading to a noise-limited indoor environment and conversely an interference-limited outdoor environment.

Firstly, in an interference-limited outdoor region, mmWave spectral efficiency $\gamma_{\mathrm{m.out}}$ is analytically represented in the following Lemma.

Lemma 2. *(Downlink Outdoor mmWave)* At U_0 when located outside indoor regions for $\lambda_{\mathrm{m}} \gg \lambda_{\mathrm{u}}$, downlink outdoor mmWave spectral efficiency $\gamma_{\mathrm{m.out}}$ is lower bounded as follows.

$$\gamma_{\mathrm{m.out}} > \log\left(1 + \frac{2\pi}{\theta}\left[\frac{e^{\lambda_g S}\lambda_{\mathrm{m}}}{\rho_{\mathrm{m}}\lambda_{\mathrm{u}}}\right]^{\frac{\alpha_{\mathrm{m}}}{2}}\right)^{1 - \sqrt{\frac{S}{\lambda_{\mathrm{m}}}}} \tag{6}$$
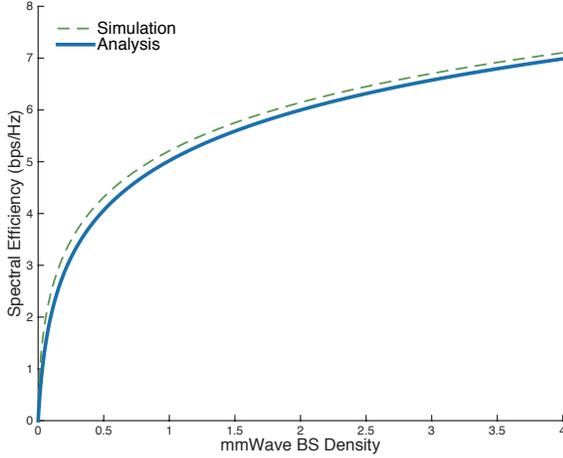
Fig. 4. Spectral efficiency of a typical *indoor* downlink mmWave user for the indoor path loss exponent is set as 2, and user density $\lambda_\mathrm{u} = 0.02$.

where $\rho_\mathrm{m} := \int_0^\infty 1/(1 + u^{\alpha_\mathrm{m}/2}) du$

The result implies BS densification not only improves SIR, but also overcomes indoor wall blockages (see the logarithm function's exponent in (6)), leading to the spectral efficiency enhancement. Increasing indoor area S decreases outdoor interference while increasing desired signal blockage effect. The latter can be fully compensated by BS densification, so larger S ensures better outdoor spectral efficiency under an ultra-dense environment. The tightness of the analytic result is numerically validated, and visualized in Fig. 3.

Secondly, in a noise-limited indoor region, mmWave spectral efficiency $\gamma_\mathrm{m.in}$ is given in the following Proposition.

Lemma 3. *(Downlink Indoor mmWave)* At U_0 when located within indoor regions for $\lambda_\mathrm{m} \gg \lambda_\mathrm{u}$, downlink indoor mmWave spectral efficiency $\gamma_\mathrm{m.in}$ is lower bounded as follows.

$$\gamma_\mathrm{m.in} > \log\left(1 + \frac{\pi\lambda_\mathrm{m}}{\sigma^2}\right) \tag{7}$$

The relationship between BS density λ_m and received power intuitively interprets the result above. The received power scales with r^{-2} for indoor mmWave path loss exponent 2 while $\mathsf{E}[r]$ in [11] scales with $1/\sqrt{\lambda_\mathrm{m}}$, resulting in the linear scaling of SNR with λ_m. The tightness of the analysis is numerically verified as shown in Fig. 4.

Combining the outdoor and indoor mmWave spectral efficiencies (Lemmas 3 and 4), the following result provides the overall downlink mmWave spectral efficiency γ_m as below.

Proposition 2. *(Downlink mmWave)* At U_0 for $\lambda_\mathrm{m} \gg \lambda_\mathrm{u}$, downlink mmWave spectral efficiency γ_m at U_0 is lower bounded as follows.

$$\gamma_\mathrm{m} > \log\left(1 + \frac{\pi\lambda_\mathrm{m}^{(\frac{\alpha_\mathrm{m}}{2}-1)e^{-\lambda_g S}+1}}{\sigma^2}\left[\frac{2\sigma^2}{\theta}\left(\frac{e^{\lambda_g S}}{\rho_\mathrm{m}\lambda_\mathrm{u}}\right)^{\frac{\alpha_\mathrm{m}}{2}}\right]^{e^{-\lambda_g S}}\right) \tag{8}$$

The result indicates mmWave downlink spectral efficiency is a logarithmic function of BS density λ_m. The exponent of λ_m shows densification is more effective when 1) outdoor mmWave attenuation is severe (large α_m) and/or 2) users are

more likely to be in outdoor region (small $\lambda_g S$). In addition, sharper beam (small θ) increases the spectral efficiency. On the other hand, the spectral efficiency decreases with user density since more users bring about larger interference.

IV. RESOURCE MANAGEMENT AND CELL PLANNING IN MILIMETER-WAVE OVERLAID ULTRA-DENSE CELLULAR NETWORKS

This section analyzes μWave resource allocation behaviors, and consequently provides the mmWave overlaid cellular network design guidelines in the perspectives of resource allocation and cell planning.

A. Downlink Average Rate with Minimum Uplink Rate Requirement

Define downlink and uplink average rates R_d and R_u as follows.

$$R_\mathrm{d} := W_{\mu.\mathrm{d}}\gamma_\mu + W_\mathrm{m}\gamma_m \tag{9}$$
$$R_\mathrm{u} := W_{\mu.\mathrm{u}}\gamma_\mu \tag{10}$$

Let $T \leq 1$ denote the minimum ratio of uplink to downlink rates. We consider the following problem:

$$\mathsf{P1}. \max_{W_\mu} R_\mathrm{d}$$

subject to

$$R_\mathrm{u}/R_\mathrm{d} \geq T \tag{11}$$
$$W_{\mu.\mathrm{d}} + W_{\mu.\mathrm{u}} = W \tag{12}$$

where $W_{\mu.\mathrm{d}}$, $W_{\mu.\mathrm{u}}$, W respectively denote downlink, uplink, and entire bandwidths. The objective function is maximized when the equality in (11) holds, leading to the following μWave downlink resource allocation.

Proposition 3. *(μWave Resource Allocation)* If $W \geq TW_\mathrm{m}\gamma_\mathrm{m}/\gamma_\mu$, the following μWave downlink resource allocation maximizes the average rate while guaranteeing the minimum uplink rate:

$$W_{\mu.\mathrm{u}}^* = \frac{T}{1+T}\left(W + \frac{W_\mathrm{m}\gamma_\mathrm{m}}{\gamma_\mu}\right) \quad \text{and}$$
$$W_{\mu.\mathrm{d}}^* = \frac{1}{1+T}\left(W - \frac{TW_\mathrm{m}\gamma_\mathrm{m}}{\gamma_\mu}\right); \tag{13}$$

where $0 \leq W_{\mu.\mathrm{d}}^*, W_{\mu.\mathrm{u}}^* \leq W$; otherwise, the minimum uplink rate requirement cannot be satisfied.

Increasing mmWave downlink rate (λ_m and/or W_m) leads to less downlink μWave allocation $W_{\mu.\mathrm{d}}^*$ and more uplink μWave allocation $W_{\mu.\mathrm{u}}^*$. The reason is because the mmWave band provides most of the downlink transmissions without the aid of μWave band, and thus all the μWave band becomes dedicated to the uplink transmissions to assure the minimum uplink rate requirement. In addition, increasing μWave resource W allows more $W_{\mu.\mathrm{d}}^*$ and $W_{\mu.\mathrm{u}}^*$, but the latter increases faster (notice $1/(1+T) \geq T/(1+T)$ for $T \leq 1$). Such uplink biased μWave resource allocation tendency is the opposite way of the current resource management trend seeking more downlink resources, to be further elucidated under practical scenarios in Section V.

Increasing μWave BS density λ_μ, on the other hand, makes the resource more prone to be allocated to downlink transmissions. Recalling μWave uplink-downlink reciprocity in Lemma 2, increasing λ_μ identically improves both uplink and downlink rates. In spite of such identical increments, the
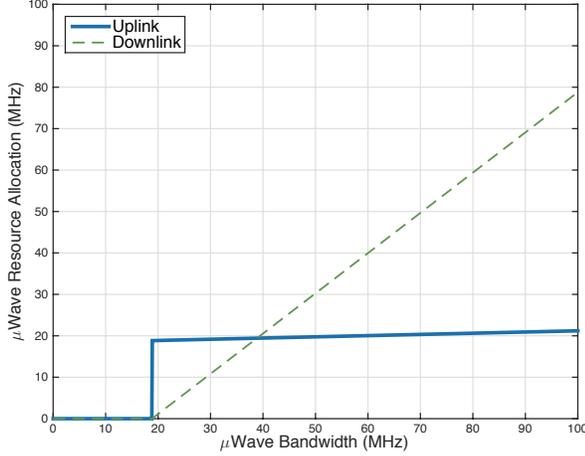
Fig. 5. Uplink and downlink μWave resource allocations with mmWave bandwidth 500 MHz ($\lambda_\mathrm{u} = 0.02$, $\alpha_\mu = 4.58$, $\alpha_\mathrm{m} = 5.76$, $\lambda_g = 0.1$, $\theta = 10°$, $\sigma^2 = 1$, $T = 0.03$).
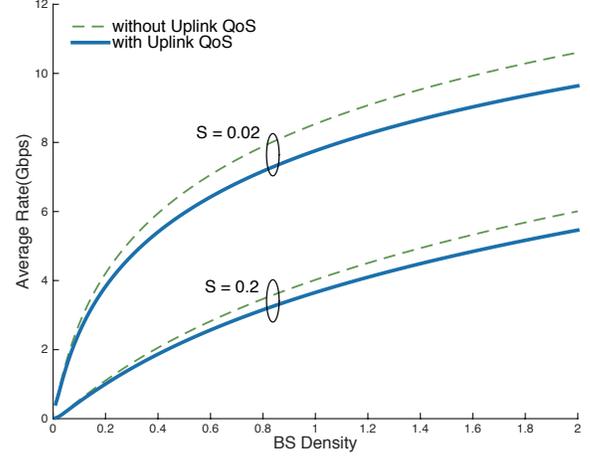

Fig. 6. Maximized downlink average rate with and without the uplink rate requirement $T = 0.1$ under μWave bandwidth 20 MHz and mmWave bandwidth 500 MHz ($\lambda_\mathrm{u} = 0.02$, $\alpha_\mu = 4.58$, $\alpha_\mathrm{m} = 5.76$, $\lambda_g = 0.1$, $\theta = 10°$, $\sigma^2 = 1$).

uplink/downlink ratio increases since the uplink rate is no larger than downlink rate. This results in increasing $W_{\mu.\mathrm{d}}$ until the equality in (11) holds.

Applying the resource allocation results to (9) yields the following uplink rate requirement guaranteeing maximized downlink average rate.

Corollary 1. *(Downlink Average Rate with Minimum Uplink Rate Requirement)* If $W \geq TW_\mathrm{m}\gamma_\mathrm{m}/\gamma_\mu$ for $\lambda_\mathrm{m}, \lambda_\mu \gg \lambda_\mathrm{u}$, maximized downlink average rate while guaranteeing the minimum uplink rate is given as:

$$R_\mathrm{d}{}^* = \frac{1}{1+T} \log\left(1 + c_\mathrm{d}\lambda_\mathrm{m}{}^{W_\mathrm{m}\left(1-\sqrt{\frac{S}{\lambda_\mathrm{m}}}\right)\left[\left(\frac{\alpha_\mathrm{m}}{2}\right)e^{-\lambda_g S}+1\right]}\lambda_\mu{}^{\frac{W\alpha_\mu}{2}}\right) \tag{14}$$

where

$$c_\mathrm{d} = \left[\frac{\pi}{\sigma^2}\left\{\frac{2\sigma^2}{\theta}\left(\rho_m e^{-\lambda_g S}\lambda_\mathrm{u}\right)^{-\frac{\alpha_\mathrm{m}}{2}}\right\}^{e^{-\lambda_g S}}\right]^{W_\mathrm{m}\left(1-\sqrt{\frac{S}{\lambda_\mathrm{m}}}\right)}(\rho_\mu\lambda_\mathrm{u})^{-\frac{\alpha_\mu W}{2}}$$

otherwise, the rate cannot satisfy the uplink rate requirement.

The result reveals BS densification logarithmically increases the downlink rate while μWave and mmWave resource amounts and path loss exponents linearly increases the rate. Larger indoor region area under $\lambda_\mathrm{m} \gg S$ exponentially decreases the rate. Additionally, increasing the minimum uplink rate target decreases the downlink rate. This result is visually elucidated by Fig. 6 in Section V.

B. Resource Management and Cell Planning

This section provides resource management and cell planning guidelines based on the closed-form μWave uplink/downlink (see Proposition 1) and mmWave downlink (see Proposition 2) spectral efficiency lower bounds derived in Sections III-B and D. As Fig. 3 and 4 numerically validate the tightness of the lower bounds, we henceforth regard these lower bounds as approximations. To simplify our exposition, we focus on the asymptotic behaviors as $\lambda_\mu, \lambda_\mathrm{m} \to \infty$.

Consider the uplink requirement feasible condition $W \geq TW_\mathrm{m}\gamma_\mathrm{m}/\gamma_\mu$ from Proposition 3, leading to the minimum

number of the required μWave BSs along with increasing mmWave BSs.

Proposition 4. *(Required μWave BS)* For $\lambda_\mu, \lambda_\mathrm{m} \to \infty$, guaranteeing the minimum uplink rate requires the following μWave and mmWave BS density relation:

$$O(\lambda_\mathrm{m}) = O\left(\lambda_\mu{}^{\frac{\alpha_\mu W}{TW_\mathrm{m}\left[(\alpha_\mathrm{m}-2)e^{-\lambda_g S}+2\right]}}\right) \tag{15}$$

To achieve the ever-growing downlink average rate while guaranteeing the minimum uplink average rate, the result shows the required μWave BS density should be increased with much higher order of the mmWave BS density in practical scenarios where $W_\mathrm{m} \gg W$. The reason is the logarithmic spectral efficiency improvement by μWave BS densification (see Proposition 1) cannot overtake the linearly increased mmWave downlink rate.

Ameliorating this situation in practice therefore requires to procure additional μWave resource as Fig. 7 visualizes in Section V. The following Corollary investigates how much amount of μWave resource is required to achieve the goal when μWave BS densification is linearly proportional to the mmWave BS's.

Corollary 2. *(Required μWave Resource)* For $\lambda_\mu \to \infty$ and $\lambda_\mathrm{m} = p\lambda_\mu$ for a constant $p > 0$, the minimum uplink average rate constraint requires μWave resource amount as follows.

$$W \geq \frac{TW_\mathrm{m}}{\alpha_\mu}\left[(\alpha_\mathrm{m}-2)e^{-\lambda_g S}+2\right] \tag{16}$$

The result insists that even when the number of μWave BSs increases with the same order of the mmWave BSs', it is imperative to procure additional μWave resource in order to increase downlink average rate with assuring the minimum uplink rate. It is visually elaborated by Fig. 5 in Section V.

V. NUMERICAL RESULTS

This section visualizes the resource management and cell planning guidelines proposed in Section IV under practical scenarios. According to [1], path loss exponents are set as:
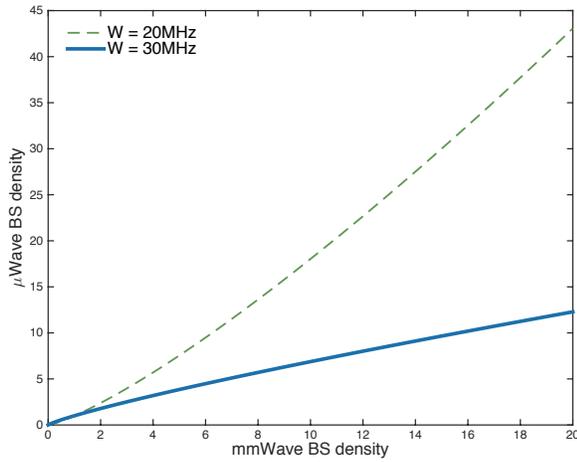
Fig. 7. Minimum required μWave BS density as mmWave BS density increases for μWave bandwidths 20 MHz and 30 MHz under mmWave bandwidth 500 MHz ($T = 0.04$, $\lambda_u = 0.02$, $\alpha_\mu = 4.58$, $\alpha_m = 5.76$, $\lambda_g = 0.1$, $S = 0.02$, $\theta = 10°$, $\sigma^2 = 1$).

$\alpha_\mu = 4.58$, $\alpha_m = 5.76$. The indoor mmWave path loss exponent is set as 2 as assumed in Section II-C. Additionally, user density $\lambda_u = 0.02$, indoor region density $\lambda_g = 0.1$, main lobe beam width $\theta = 10°$, and noise power σ^2 is fixed as 1. The radio resource amount for μWave is set as 20 MHz as default, and the amount for mmWave as 500 MHz [6].

Fig. 5 illustrates Proposition 3 and Corollary 2 that shows the uplink (thick blue) and downlink (thin green) μWave resource allocations. For the given environment, guaranteeing the uplink average rate by 3% of the downlink rate requires at least 19 MHz uplink μWave bandwidth. Considering the current 20 MHz μWave bandwidth, It implies implies even achieving such low uplink/downlink ratio requires to dedicate most of the μWave bandwidth to the uplink due to severe uplink/downlink rate asymmetry. This contradicts with the current resource allocation tendency that is likely to allocate more resource to downlink [7]. Focusing on the curve slopes once the minimum uplink rate requirement is achieved, it shows the surplus μWave bandwidths are mostly allocated to the downlinks so as to maximize the downlink rates.

Fig. 6 corresponds to Corollary 1 that illustrates the maximized downlink rate with assuring the minimum uplink/downlink rate ratio T along with increasing mmWave BS density λ_m. The figure compares the effect of the uplink rate requirement on the resultant downlink rate (solid versus dashed), capturing the downlink rate is pared down to the point achieving the minimum uplink rate. Moreover, the figure revels the effect of the indoor region area S (blue versus green) that larger S leads to the lower downlink rate as expected in the discussion of Corollary 1. In addition, the figure reveals that 1 Gbps downlink average rate is achieved when mmWave BS density is 1.5 times larger than the user density for $S = 0.02$ and when it is 10 times larger for $S = 0.2$.

Fig. 7 visualizes Proposition 4 that validates the proposed resource management and cell planning guidelines. It shows μWave BS densification cannot independently cope with the uplink rate requirement problem, but requires the aid of procuring more μWave spectrum. The impact of procuring more μWave spectrum is observed by the curve increasing tendencies in the figure. The μWave BS density for μWave

bandwidth 20 MHz (dotted green) shows power-law increase while the density for 30 MHz (solid blue) does sub-linear increase. These different required μWave BS increasing rates corroborate the necessity of the additional μWave spectrum. The figure in addition reveals that the effect of indoor region area S that decreases the minimum required μWave BS density due to its downlink rate reduction discussed in Corollary 1 and visualized in Fig. 6.

VI. CONCLUSION

In this paper we propose a mmWave overlaid ultra-dense cellular network operating downlink transmissions via both mmWave and μWave bands whereas uplink transmissions only via μWave band due to its technical implementation difficulty at mobile users. Regarding this asymmetric uplink and downlink structure, we provide the resource management and cell planning guidelines so as to maximize downlink average rate while guaranteeing the minimum uplink rate (see Propositions 3 and 4 as well as Corollary 2). Such results are calculated on the basis of the closed-form mmWave (see Proposition 1) and μWave (see Proposition 2) spectral efficiencies derived by using stochastic geometry.

The weakness of this study is the use of an arbitrary indoor region (or blockage) area S when calculating mmWave spectral efficiencies, which may alter the network design results. Moreover, the blockage modeling in this paper is necessary to be compared with the recent mmW blockage analysis such as [12], [13]. Further extension should therefore contemplate more realistic building statistics as well as a rigorous comparison with the preceding works.

REFERENCES

[1] T. S. Rappaport, S. Sun, R. Mayzus, H. Zhao, Y. Azar, K. Wang, G. N. Wong, J. K. Schulz, M. Sammi, and F. Gutierrez, "Milimeter Wave Mobile Communications for 5G Cellular: It Will Work!," *IEEE Access*, vol. 1, pp. 335–349, 2013.
[2] Z. Pi and F. Khan, "An Introduction to Milimeter-Wave Mobile Broadband Systems," *IEEE Communications Magazine*, vol. 49, no. 6, pp. 101–107, 2011.
[3] J. G. Andrews, S. Buzzi, W. Choi, S. Hanly, A. Lozano, A. C. K. Soong, and J. C. Zhang, "What Will 5G Be?," *IEEE Journal on Selected Areas in Communications*, vol. PP, June 2014.
[4] I. Hwang, B. Song, and S. S. Soliman, "A Holistic View on Hyper-Dense Heterogeneous and Small Cell Networks," *IEEE Communications Magazine*, vol. 51, no. 6, pp. 20–27, 2013.
[5] J. Park, S.-L. Kim, and J. Zander, "Asymptotic Behavior of Ultra-Dense Cellular Networks and Its Economic Impact," *in Proc. IEEE Global Communications Conference (GLOBECOM 2014), Austin, United Sates*, December 2014.
[6] T. Kim, J. Park, J.-Y. Seol, S. Jeong, J. Cho, and W. Roh, "Tens of Gbps Support with mmWave Beamforming Systems for Next Generation Communications," *Proc. IEEE Global Communications Conference (GLOBECOM 2014)*, pp. 3685–3690, 2013.
[7] D. Astely, E. Dahlman, G. Fodor, S. Parkvall, and J. Sachs, "LTE Release 12 and Beyond," *IEEE Communications Magazine*, vol. 51, pp. 154–160, July 2013.
[8] Ericsson, "Ericsson Mobility Report," November 2012.
[9] P. Hall, *Introduction to the Theory of Coverage Processes*. Wiley, 1988.
[10] S. M. Yu and S.-L. Kim, "Downlink Capacity and Base Station Density in Cellular Networks," *Proc. IEEE WiOpt Workshop on Spatial Stochastic Models for Wireless Networks (SpaSWiN 2013)*, May 2013.
[11] D. Stoyan, W. S. Kendall, and J. Mecke, *Stochastic Gemoetry and its Applications*. Wiley, 2nd ed., 1995.
[12] T. Bai, R. Vaze, and R. W. Heath, Jr, "Analysis of Blockage Effects on Urban Cellular Networks," *IEEE Transactions on Wireless Communications*, vol. 13, no. 9, pp. 5070–5083, 2014.
[13] M. N. Kulkarni, S. Singh, and J. G. Andrews, "Coverage and Rate Trends in Dense Urban mmWave Cellular Networks," *in Proc. IEEE Global Communications Conference (GLOBECOM 2014), Austin, United Sates*, December 2014.